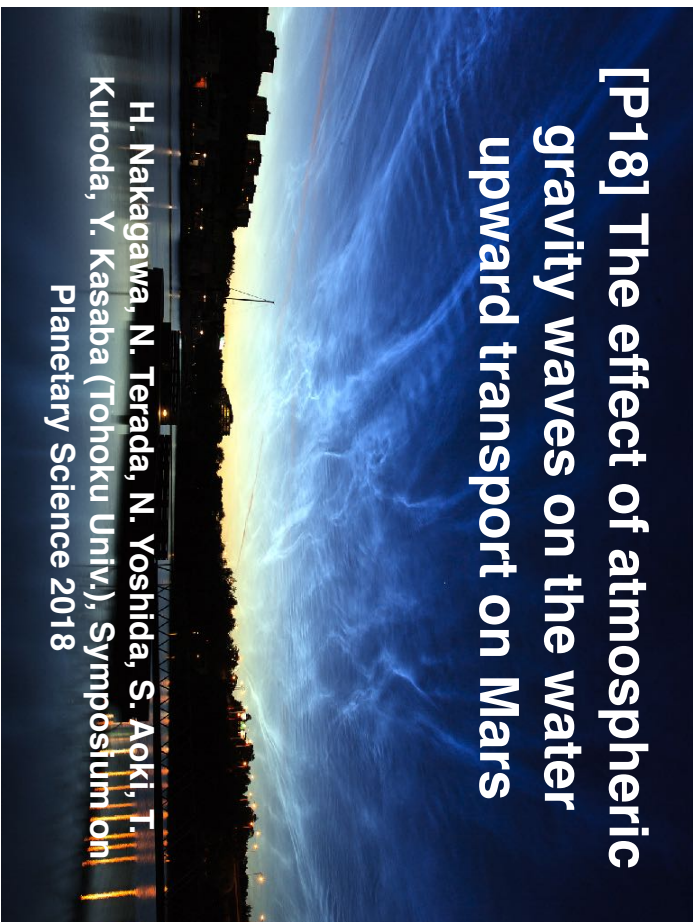


# [P18] The effect of atmospheric gravity waves on the water upward transport on Mars

H. Nakagawa, N. Terada, N. Yoshida, S. Aoki, T. Kuroda, Y. Kasaba (Tohoku Univ.), Symposium on Planetary Science 2018



## 1-2 Wavelike perturbations on Mars

- Wavelike perturbations **ubiquitously exist** on Mars as well.
- **Larger amplitudes** (10 times than Earth) [Terada+17] could have on the effects in the Martian atmosphere.
- The effect of these waves have not been properly addressed.

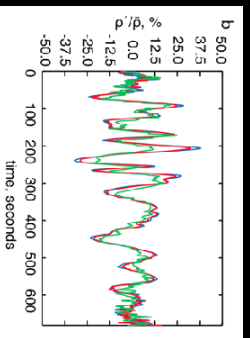


Fig. [England+17].

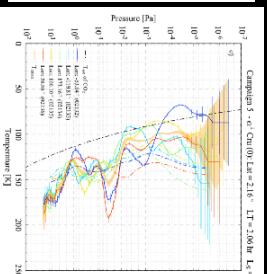


Fig. [Groller+].

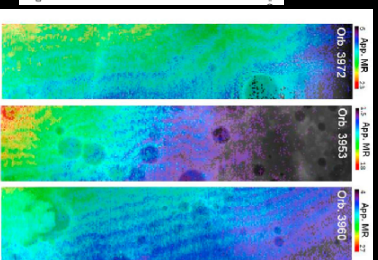


Fig. [Alieri+12].

3

## 1-1 GW and its role

- It is now widely recognized that atmospheric gravity waves (GWs) in the lower atmosphere play an important role in the terrestrial mesosphere and thermosphere. They affect the **dynamics, composition, and thermal structure** [Fritts and Alexander, 2003].
- GWs excited by flow over topography, instabilities of jets, convections.

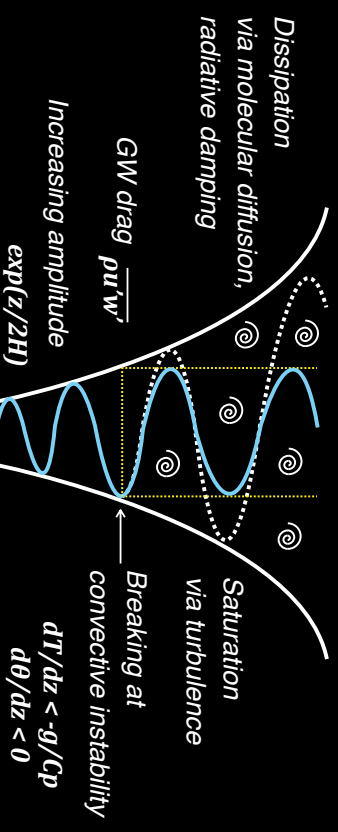


Fig. Schematic drawing of upward propagating waves.

2

## 1-3 Unexpected water loss at perihelion

- Short-term variations (weeks-months) in H escape [Clarke+17]
- Water vapor layer above 40km altitude [Maltagliati+13]
- Weeks variations can have on planetary evolution [Chaffin+17]
- Both happens at the perihelion which has a substantial increase of surface temperature and dust opacity, which leads GW activity.

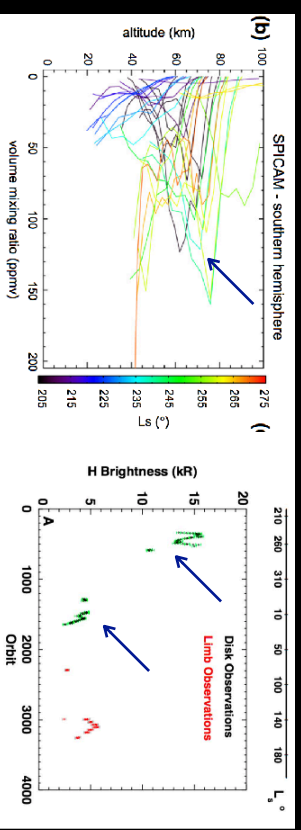


Fig. The vertical profiles of water vapor [Maltagliati+13] and hydrogen coronal emission intensity [Clarke+17].

4

## 1-4 Water cycle on Mars

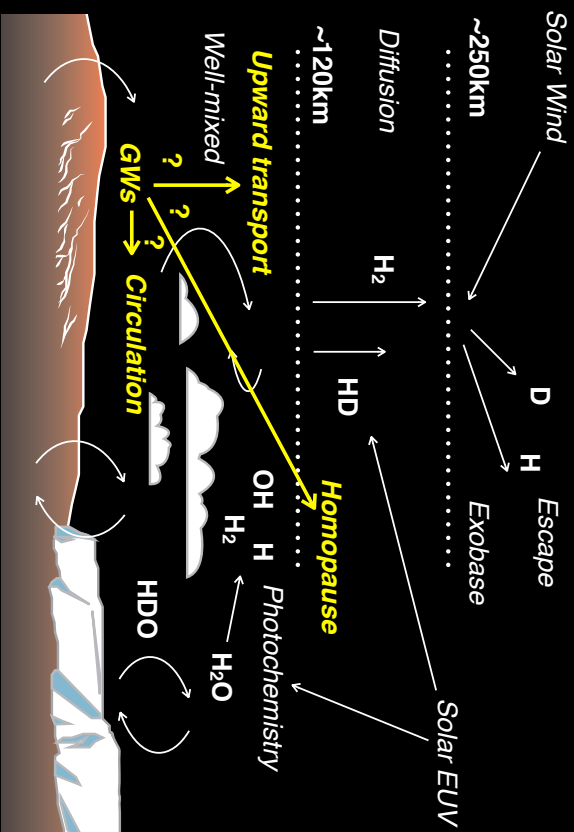


Fig. Schematic drawing of the martian water cycle [Nakagawa, under review].

5

## 1-5 Purpose of this study



- Remote sensing by IUVS provide opportunities for investigating possible links of the atmospheric waves between troposphere and thermosphere on Mars.
- We use the IUVS stellar occultation measurements to **characterize a global distribution of wave-like perturbations** in mesosphere (50-80km) and lower thermosphere (100-130km).
- The **convective instability** related to the wave-like perturbations, and the **homopause height** are simultaneously addressed in order to investigate the effect of the waves on the water cycle on Mars.

## 2-1 Observation

- We use MAVEN/IUVS stellar occultation data.
- 12 campaigns, ~200 profiles, in March 2015 and January 2017.
- It covers **30 to 150km** altitude range w/ **2-10km** high-vertical resolution.

6

## 2-2 Data set



- CO<sub>2</sub>, Temperature, O<sub>2</sub> and aerosols (τ)
- Wave data criteria: vertical resolution < 5km, vertical coverage > 20km.

Tab. List of the stellar occultation campaigns.

#	Date	Orbit	L <sub>s</sub>	Used
1	24-26 Mar 2015	935-944	315	4
2	17-18 May 2015	1222-1226	344	0
3	1-2 Aug 2015	1635-1640	22	17
4	22-23 Sep 2015	1911-1916	45	0
5	3-4 Nov 2015	2132-2137	64	13
6	18-19 Jan 2016	2533-3838	97	3
7	17-18 Mar 2016	2848-2853	124	7
8	26-27 May 2016	3223-3228	159	8
9	14-15 Jul 2016	3498-3493	186	3
10	21-22 Sep 2016	3856-3861	227	0
11	16-18 Nov 2016	4146-4155	262	37
12	11-12 Jan 2017	4436-4445	297	8

7

## 2-3 Data coverage

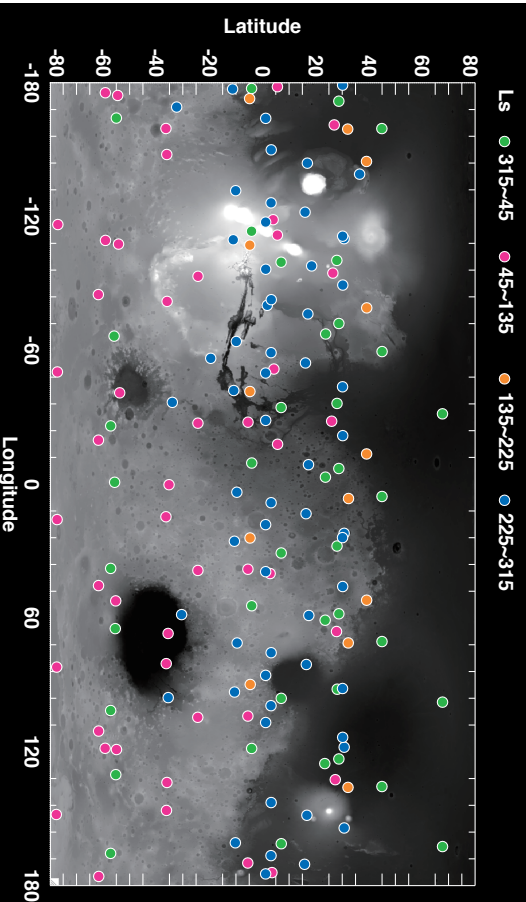


Fig. Foot-prints of the occultation measurements.

8

## 2-4 Temperature profiles



- Large-scale ( $\lambda_z \sim 30-40\text{km}$ ) waves, assumed to be thermal tides.
- Possibility of convective instability by wave breaking of tides alone.

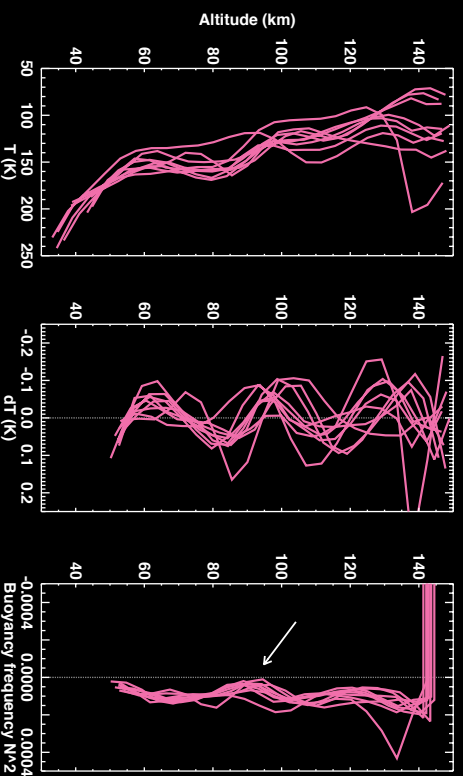


Fig. Example of profiles at Ls297, lat3N (HR3206 Gam1 Vel).

9

## 2-4 Temperature profiles 2



- Small-scale ( $\lambda_z \sim 10-20\text{km}$ ) waves, assumed to be GWs ( $\Delta T = 10-20\%$ ).
- **Much more convective instabilities** by interaction between tides & GWs.

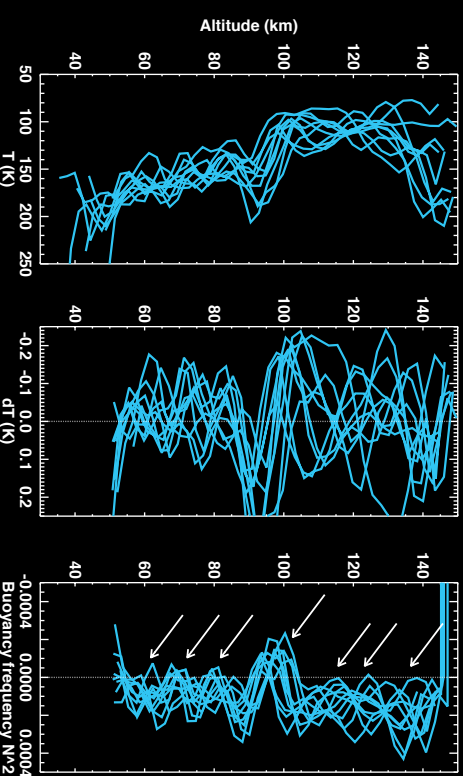


Fig. Example of profiles at Ls262, lat8S (HR6165 23tau Sco).

10

## 2-5 Convective Instability



- Possible to much more breaking in 40-100km at perihelion

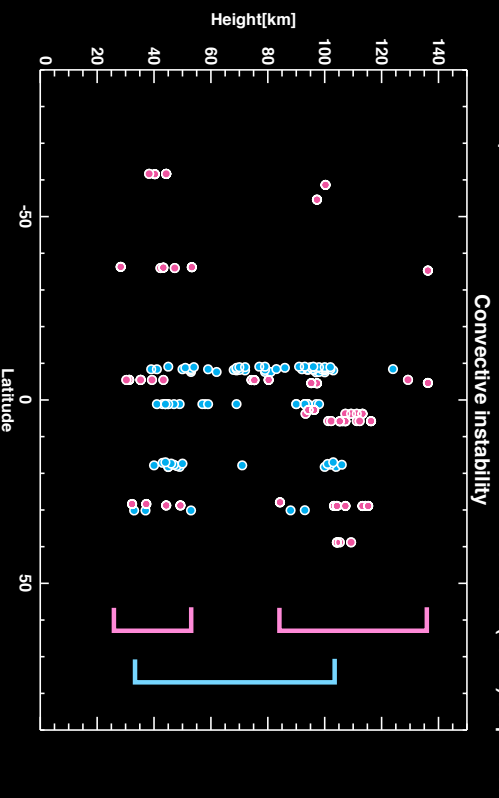


Fig. Lat-alt distribution of the convective instability ( $N^2 < 0$ ).

11

## 2-6 Latitudinal dependence of dT



- Larger dT in **summer** hemisphere, in particular at perihelion.

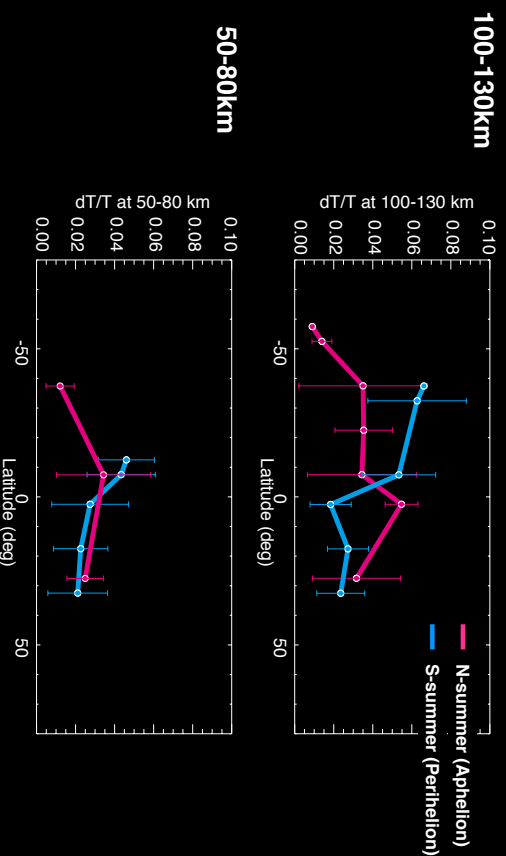


Fig. Zonal-averaged dT along latitudes (the deviation of zonal-mean for bars).

12

### 3-1 Homopause height ( $O_2/CO_2$ )



- Assume  $O_2/CO_2 = 2.0 \times 10^{-3}$  on the surface [cf.  $1.45 \times 10^{-3}$  in Mahafy+13]
- $O_2/CO_2 > 115\text{km}$  to extrapolate the homopause height ( $O_2$  obtained only from FUV channel  $> 110\text{km}$ )

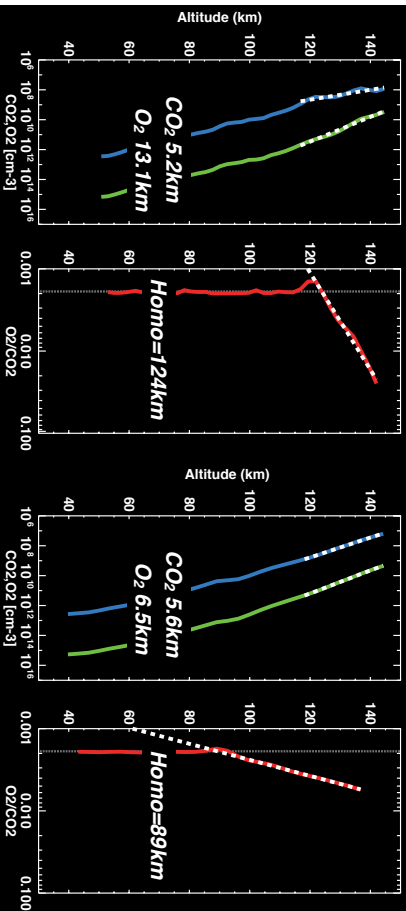


Fig. Profiles of  $CO_2$  &  $O_2$  number density, and  $O_2/CO_2$  (left: Ion25.3, lat7.2S, LT24, orbit#4152, right: Ion-26.7, lat1.1N, LT23, orbit#4153 in Nov. 2016).

### 3-2 Homopause vs Waves



- The homopause height mainly found at 90-120km in both seasons.
- Larger amplitudes of waves corresponds to higher homopause?

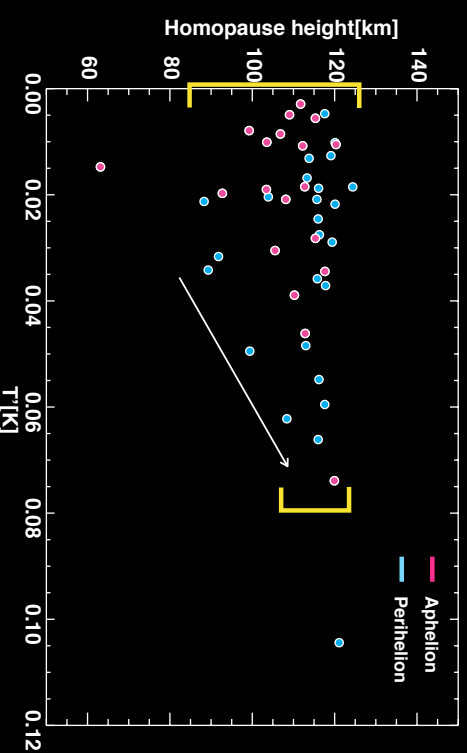


Fig.

### 3-3 Homopause vs Aerosol (40-80km)

- Larger  $\tau$  of aerosols in 40-80km at perihelion.
- Larger  $\tau$  in 40-80km corresponds to higher homopause.

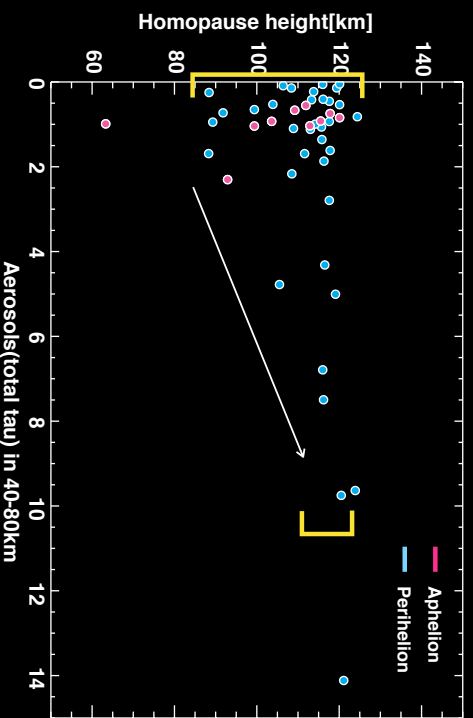


Fig.

### 4-1 Discussion ~ GWS drag



- GWS drag to accelerate the meridional circulation, which affect on the transport from Southern to Northern hemisphere at high alt. (~150km).
- GWS drag in lower alt. (40-80km) at high dust opacity [Kuroda+09].

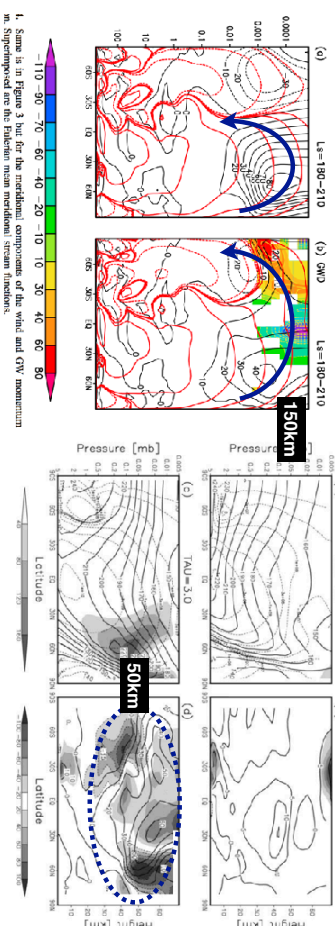


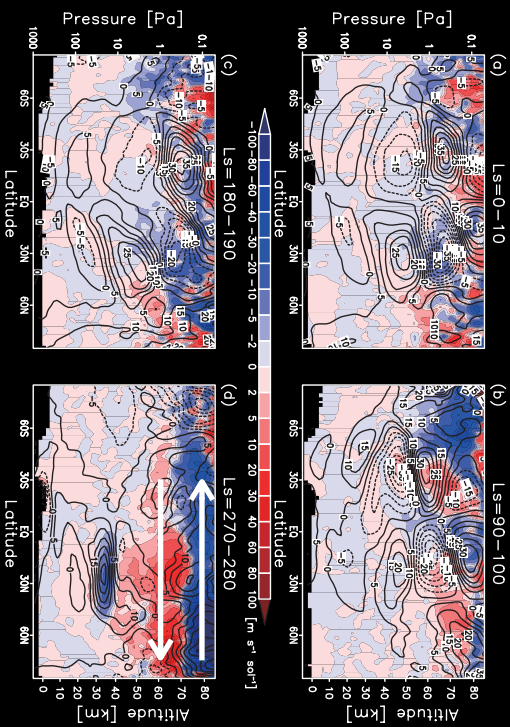
Fig. 1. Results of simulations for the "low dust" ( $\tau = 0.5$ ) run (upper panels), and the "strong dust" ( $\tau = 3.0$ ) lower panels; (e) and (f) The zonal dust temperature [K] (red lines), meridional mass stream rate [K and  $10^{18}$  molecules], (g) and (h) The zonal dust temperature [K] (red lines), meridional mass stream rate [K and  $10^{18}$  molecules], (i) and (j) The meridional velocity [m s $^{-1}$ ] (contour) and ER the divergence  $\nabla \cdot \mathbf{V}$  [m s $^{-1}$  s $^{-1}$ ] (shaded, negative values are surrounded by thin dashed lines).

Fig. [Medvedev+11; Kuroda+09]

## 4-2 Discussion ~ GWS drag



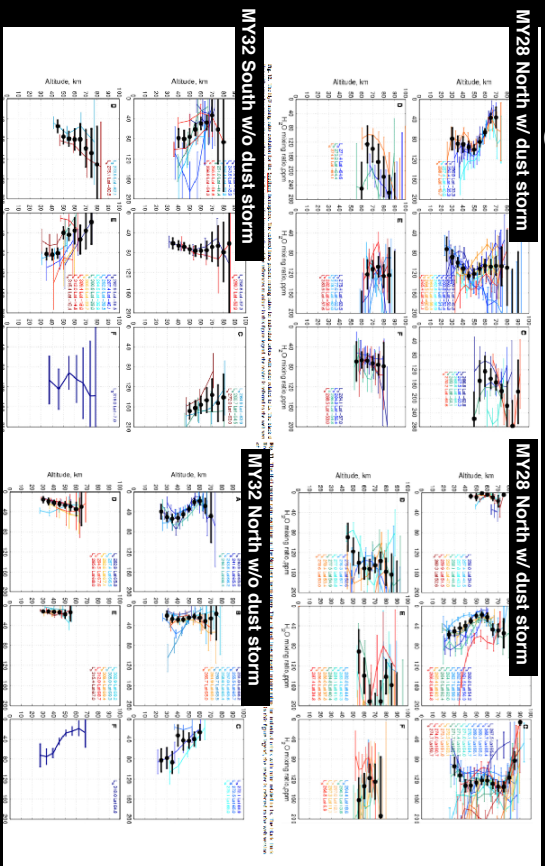
$$-1/\rho * d(\rho v'w')/dz \text{ and } \bar{v} \text{ by GW (s=61-106)}$$



• Mass transport over hemispheres could be achieved only at perihelion.

Fig. The GWS drag in meridional circulations.

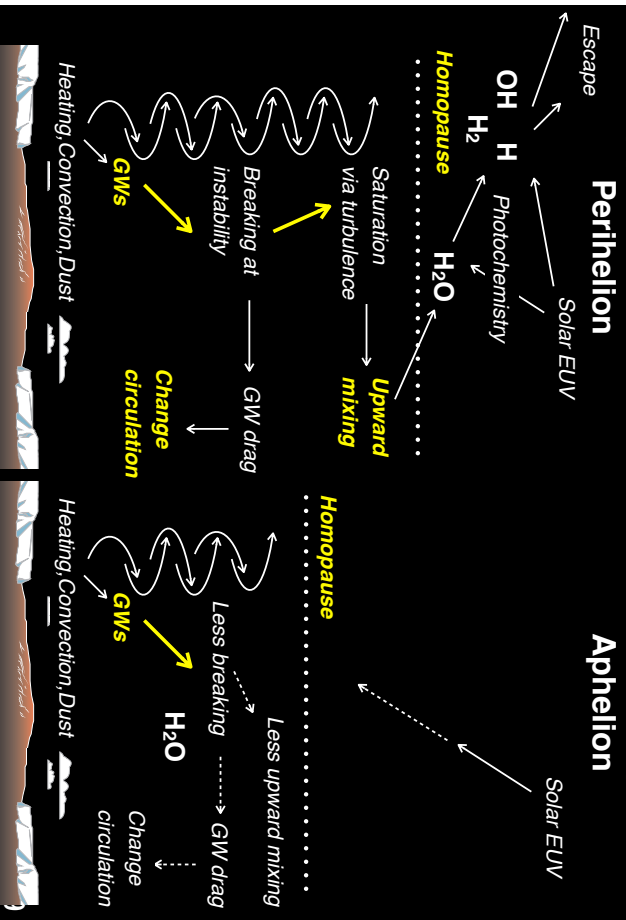
## 4-3 High-alt. H<sub>2</sub>O w/, w/o dust storm



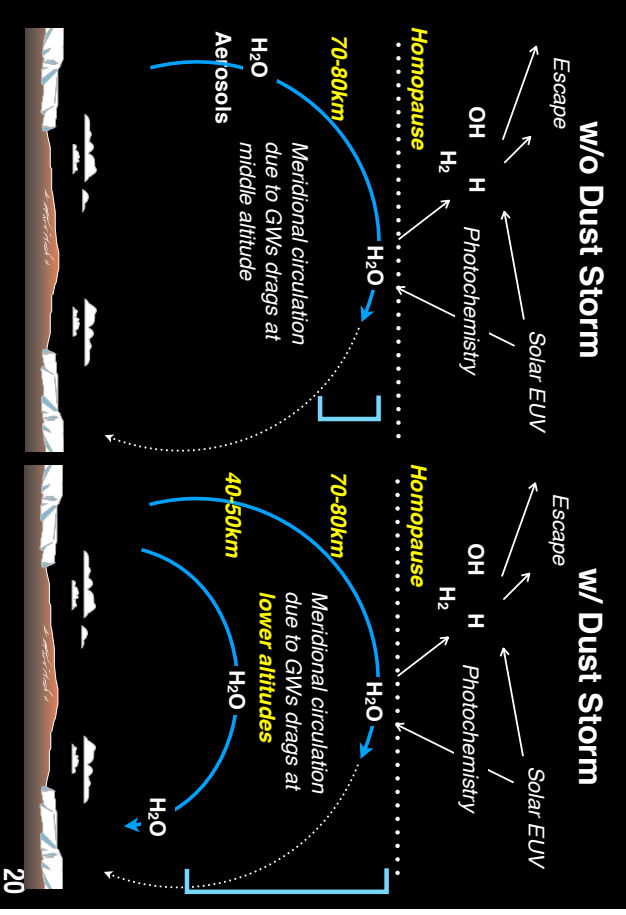
• No increase in the N-hemisphere in MY32 (No transport from south?).

Fig. from [Fedorova+18]

## 4-4 Hypothesis: Waves and water cycle



## 4-5 Hypothesis: Waves and water cycle



## 5. Summary



- **Small-scale ( $\lambda_p \sim 10\text{-}20\text{km}$ ) waves**, assumed to be GWs ( $\Delta T = 10\text{-}20\%$ ) in the temperature profiles derived from MAVEN/UVS occultations.
- **Larger wave activity in summer hemisphere** (in particular at perihelion), which is quite different from that in the Earth's atmosphere.
- Reasonably agreement with MGCM in the lower thermosphere. It suggests the observed wave structures could be explained by **the vertical propagation of GWs of tropospheric origin**.
- **Convective instabilities**, which implies the saturation (breaking) = GWs drag (change the circulation) and turbulence (well-mixing), widely found in mesosphere and lower thermosphere. Much more drag in 40-100km at perihelion, which potentially imply the acceleration of meridional circulation at the altitude, providing the transported water from the southern hemisphere to high northern hemisphere.
- Certain degree of correlation between wave activity, homopause height, and aerosol opacity in the middle atmosphere. **Water vapor might be able to transported to higher altitudes at higher homopause**, where its photodissociation rate by solar UV increase, providing an additional source of hydrogen for the upper atmosphere.
- **The well-mixing and upward transport of water vapor, and the acceleration of meridional circulation due to GWs breaking (drag) may have an important role on both the unexpected high-altitude water vapor and hydrogen escape.**